Dear Reviewer,

We sincerely thank you for your thorough and constructive review of our manuscript. Your comments have greatly helped us identify key areas that required clarification and improvement. We have carefully revised the manuscript in response to all your suggestions. Below, we provide a point-by-point reply, detailing the changes made and the corresponding locations in the revised manuscript. All major methodological explanations, theoretical background, and figure revisions have been substantially strengthened according to your feedback.

Q1- The article focuses on DSDs with different modes—unimodal, bimodal, and trimodal. However, after reading the introduction, I am still unclear on what the three modes of a fog DSD refer to, the underlying physics driving their development, and why the modes center on the highlighted diameters. Since the study emphasizes the identification and implications of DSD modes, the authors should provide more theoretical discussion and relevant literature on fog DSDs.

Answer: Thank you for the suggestion. Following your advice, we have expanded the *Introduction* in the revised manuscript to include additional content on DSD and its multimodal characteristics to strengthen the scientific background of this work. This includes a description of unimodal, bimodal, and trimodal DSDs, findings of previous observations of multimodal DSDs, the influence of DSD on fog optical properties and radiation, and the importance of representing DSD in fog numerical forecasting. For example:

About description of unimodal, bimodal, and trimodal DSDs:

"*Fog droplet size distributions (DSDs) often exhibit one or more distinct peaks, referred to as unimodal, bimodal, or trimodal DSD, and can be attributed to different origins of the fog and processes within it (Elias et al., 2015; Hammer et al., 2014; Sampurno Bruijnzeel et al., 2005).*"

About findings of previous observations of multimodal DSDs:

"*KUNKEL (1982) finds various shapes in DSDs measured in advection fogs. Many other studies have shown the existence of bimodal DSDs in mature radiation fogs (Meyer et al., 1980; Pinnick et al., 1978; Roach et al., 1976; Wendisch et al., 1998). Gultepe and Milbrandt (2007) reported DSD modes near 4 and 23 μm during winter fog events in the Toronto region. Boudala et al. (2022) investigated the seasonal and microphysical characteristics of fog at Cold Lake Airport in northern Alberta, Canada, and found that radiation fog exhibited a bimodal droplet spectrum with peaks at 4 μm and 17-25 μm.*"

About the influence of DSD on fog optical properties and radiation:

"*Stewart and Essenwanger (1982) showed that the attenuation of electromagnetic radiation by fog depends sensitively on the shape of the droplet size distribution. The DSD and water vapor determine the overall optical properties of fog and its effects on visibility and radiative transfer together.*"

About the importance of representing DSD in fog numerical forecasting:

"*The simulated evolution of fog exhibits a sensitivity to the shape of the DSD comparable to its sensitivity to aerosol loading or cloud droplet number concentration (CDNC), however it remains one of the least investigated and rarely adjusted components of microphysical parameterization schemes(Boutle et al., 2022).*"

Q2- Most results in Sections 3.2 and 3.3 rely on identifying multimodal DSDs, yet these modes often appear to be determined by the behavior of a single size bin. This raises concerns about sampling errors, which the authors have not adequately addressed. They briefly mention using local

minima to quantify the number of PSD modes, but the cited reference appears to distinguish only between unimodal and bimodal DSDs. Furthermore, the role of time averaging is not discussed in the data section, and the fact that results are based on 5-minute averages is only noted in figure captions. A better discussion of how the multimodal DSDs are defined and distinguished is necessary.

Answer: We appreciate this important concern. In the revised manuscript, we clarified the procedure used to determine the number of DSD peak modes and their peak diameters. Each fog DSD was sequentially fitted with unimodal (i=1), bimodal (i=2), and trimodal (i=3) gamma and lognormal distributions as show below:

For the gamma distribution:

$n(D) = \sum_{i=1}^{3} n_i(D) = \sum_{i=1}^{3} N_{0,i} D^{\mu_i} e^{-\lambda_i D}$

For the lognormal distribution:

$$n(D) = \sum_{i=1}^{3} n_i(D) = \sum_{i=1}^{3} \frac{n_i}{2\pi^{1/2} D_i ln\sigma_{g,i}} \exp\left(-\frac{(lnD_i - lnD_{g,i})^2}{2(ln\sigma_{g,i})^2}\right)$$

By setting the derivative to zero and solving, the peak diameter (D_{peak}) can be expressed as a function of the fitting parameter D_g and σ_g:

$D_{peak} = D_g \exp\left(-(ln\sigma_g)^2\right)$

We fitted the observed DSDs with unimodal, bimodal, and trimodal gamma and lognormal distributions. For each DSD, unimodal, bimodal, and trimodal fits using both the gamma and lognormal distribution were evaluated. The Akaike Information Criterion (AIC) and the Bayesian Information Criterion (BIC) were used to determine which of the three fits provides the best representation of the given DSD within each distribution type, and this fit was considered as the optimal fit. AIC provides a numerical basis for ranking competing models by their information loss in approximating the unknown true process, with the model yielding the lowest AIC considered the best approximating model (Symonds and Moussalli, 2011). BIC is consistent in the sense that it selects the true model with probability approaching one. A lower BIC corresponds to a higher posterior probability for the model and is therefore regarded as indicating a better model (Chakrabarti and Ghosh, 2011). Within each distribution type, the unimodal, bimodal, and trimodal fits are compared, and the one with the lowest AIC and BIC was considered the optimal fit of the given DSD.

We then retrieved N_f, LWC, R_v and R_{eff} from the optimal gamma and lognormal fits and compared them with the observations. The lognormal function provided a more accurate representation of the DSDs, so we used it to determine the number of peak modes and peak diameters in this study, and we reclassified all fog cases accordingly. The detailed formulas, calculation procedures, figures and descriptions of AIC and BIC are provided in Section 2 (*Data Set and Methods*).

We have also added a discussion on the 1-min and 5-min temporal resolutions at the end of Section 2 (*Data and Methods*) in the revised manuscript. We fitted the DSDs at both resolutions, derived the peak mode numbers and peak diameters, and reclassified all fog cases accordingly. The results show that the determination of peak mode numbers and peak diameters of DSD is not sensitive to temporal resolution, with only minor differences between the two. To reduce noise, we adopt the 5-min resolution in this study. The detailed classifications and modal diameters for both resolutions are provided in Table A2 in the appendix.

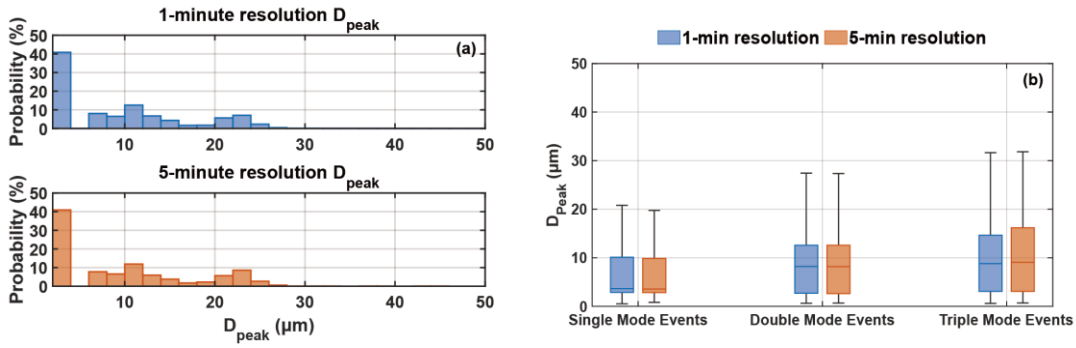

Figure 2 (a) The D_{peak} distributions of all DSDs at 1-min and 5-min resolution, and (b) the D_{peak} distributions by fog type at both resolutions

Q3- I find the interpretation of results in Section 3.2 difficult to follow. Figures 2b, d, f, and h contain overlapping DSDs in multiple colors that are not consistently referenced in the results or discussion. I recommend highlighting only the DSDs relevant to the discussion and removing or de-emphasizing distracting information.

Answer: Thank you for highlighting this readability issue. We have redesigned the figures to improve clarity. In the revised version, we selected a subset of DSDs based on the evolution of the fog life cycle. The time marked in the physical-variable time series (a) correspond exactly in number and color to the DSD spectrum (b). This mapping highlights how the DSD evolves through the fog life cycle and avoids overlap issues. For example:

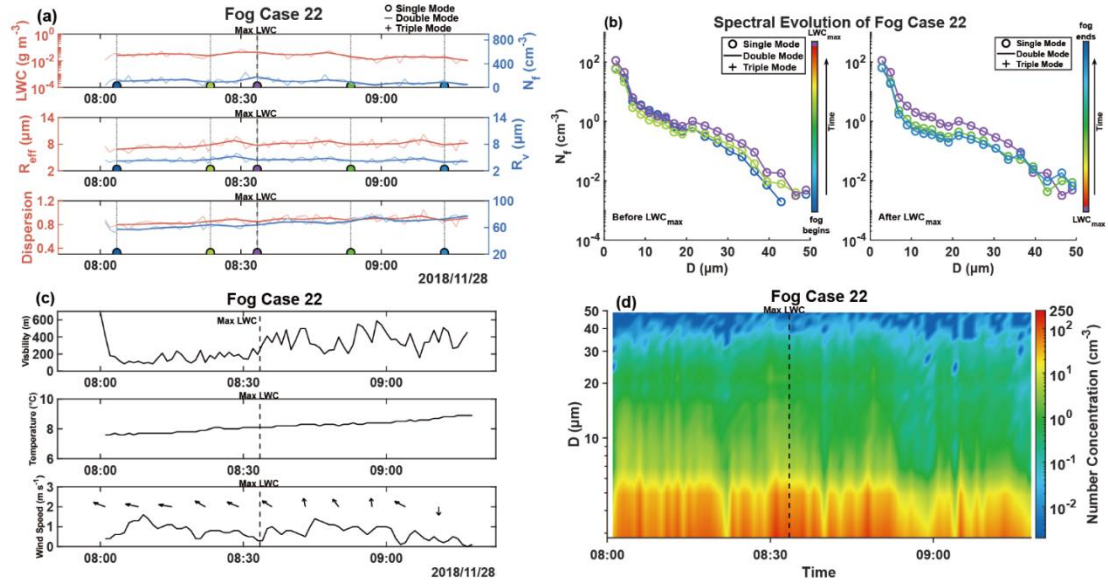

Figure 4 (a) is the temporal evolution of N_f, LWC, R_v, R_{eff}, FBS and dispersion for fog case 22, the dark lines represent 5-minute averaged values while the light lines are 1-minute averaged values. (b) is the 5-minute average DSD. As LWC reaches its maximum, the colors vary from blue to red, and each DSD in (b) are marked by colored dots in (a) with each color corresponding to a specific DSD and its number of peaks indicated. (c) is the temporal evolution of visibility, temperature and wind speed, with wind direction represented by wind barbs. (d) is the 1-minute temporal evolution of DSDs.

Q4- Section 3.4 compares a triply partitioned PDF fit-implicitly tied to the three modes of fog DSDs-to that of a single gamma distribution. However, a major null hypothesis remains unaddressed: any

DSD is likely to be better represented by a partitioned PDF than a single PDF, particularly when large DSDs (which may be assigned as trimodal) are examined. The authors should test their partition points against arbitrary alternatives to demonstrate that the observed improvements are physically meaningful and not simply an artifact of partitioning.

Answer: Thank you for point out this issue. In the revised manuscript, we discuss whether the segmentation at 10 and 22 μm has physical significance. The specific analysis is as follows:

"*To demonstrate that the superior performance of the three-segment gamma and lognormal fitting is due to the physically meaningful segmentation based on the characteristics of DSDs, rather than merely the increased number of segments, we evaluated the performance of alternative segmented fitting. Since the gamma and lognormal distributions are nonlinear, two fitting points would fall on a straight line and cannot uniquely constrain the curvature of the distribution, potentially leading to non-identifiable or ill-posed parameter estimates. Therefore, the segmentation points must satisfy two conditions: the full spectrum must be divided into three segments, and each segment must contain at least three bins. Under these constraints, 66 feasible segmentation combinations exist. Using each set of segmentation points, we performed gamma and lognormal fits for all DSDs and retrieved the corresponding* N_f, *LWC,* R_v, *and* R_{eff}. *The absolute deviations between the retrieved values and the observed ones were compared for both the alternative fittings and the fixed 10 μm and 22 μm segmentation (Figure 13). For all four microphysical parameters, the deviations from the fixed-segmentation fitting are significantly smaller than those from alternative segmentation. A two-sided binomial test was conducted to evaluate the probability that the fixed segmentation outperforms the alternative segmentation. For both distributions, the 95% confidence interval is [0.986, 1.000] with a p-value of 2.23e-308. These p-values are far below the 0.05 significance threshold. These results confirm the effectiveness of the 10 μm and 22 μm segmentation for both gamma and lognormal distribution.*"

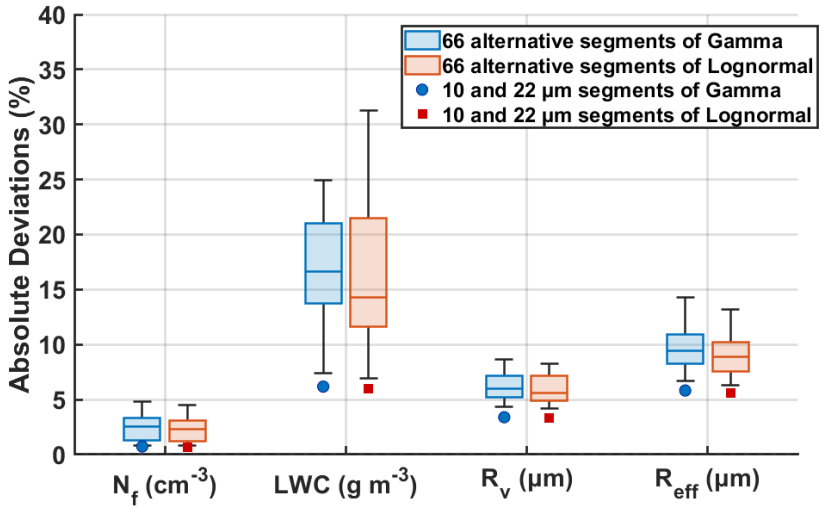

***Figure 13 Boxplots of the mean absolute deviations from 66 alternative segmented fittings, with red dots indicating the mean deviations from the fixed 10 μm and 22 μm segmentation*"**

Q5- I am also uncertain about the gamma PDF fitting methodology used in this section. In Figure 5a, the "gamma fit" appears indistinguishable from an exponential distribution. Since the gamma DSD is inherently multimodal—limiting to a power law for small particles and an exponential form for larger particles—it is unclear why the fit reduces to a simple exponential capturing only a handful of data points. A gamma PDF with a negative μ parameter would typically capture the tail behavior

more effectively. My impression is that the authors restricted μ > 0, but no explanation of the fitting procedure or parameter constraints is provided, which is also an issue.

Answer: Thank you for this crucial point. During the gamma fitting of the mean spectrum, we set the lower bounds of N_0, μ, and λ to 0, −10, and 0, respectively, and did not impose μ > 0. In our fitted mean spectrum, μ is indeed negative (-2.61×10^{-7}). In another study of winter fog in Nanjing (Wang Y, Lu C, Niu S, et al. Diverse dispersion effects and parameterization of relative dispersion in urban fog in eastern China[J]. Journal of Geophysical Research: Atmospheres, 2023, 128(6): e2022JD037514.), we also found that the gamma distribution provides a poor fit to the mean fog spectrum.

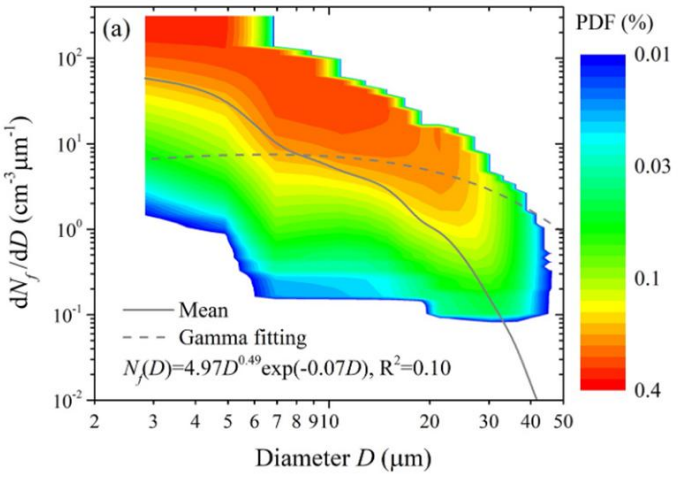

Figure 9. (a) Probability density function (PDF) of the relationship between the fog droplet number concentration (dN_f/dD) and droplet diameter (D). The gray line is the mean fog droplet number size distribution (FDSD) and the dash line is the Gamma fitting of the FDSD.

Q6- Some final opinions on the structure of the paper, but these aren't science related. Lines 124–127 should be research questions in the introduction, and the discussion section is unnecessary in it's current form since the two paragraphs could be moved to the introduction and conclusion.

Answer: We appreciate this structural advice. In the revised manuscript, we have deleted the discussion section and revised the conclusion section. New conclusion section as follows:

"As a key parameter of fog microphysical processes, the droplet size distribution (DSD) is influenced by multiple macro- and micro-scale factors, exhibits significant temporal and spatial variability, and evolves throughout the fog lifecycle, thereby posing challenges for accurate fog prediction (Niu et al., 2012; Nelli et al., 2024). Recent study has shown fog sensitivity to the shape of the DSD in models (Boutle et al., 2022). In microphysical schemes of numerical model, the gamma and lognormal distribution is widely used to represent size distributions of cloud or fog droplets, making its accuracy critical for reliable simulations.

This study investigates the microphysical characteristics of 27 winter fog events in Nanjing under polluted conditions, with a focus on the evolution of droplet size distributions (DSDs) throughout the fog lifecycle and on the application of segmented gamma fitting to the mean DSD for improved parameterization. The average N_f, LWC, R_v and R_{eff} vary over the ranges of 25-587 cm^{-3}, 0-0.28 g m^{-3}, 1.6-6 μm, 1.9-8.3 μm respectively, which shows greater N_f, lower LWC and smaller droplets comparing to other clean regions such as the tropical rainforests of southwestern China (Wang et al., 2021). Among the 27 fog cases, DSDs with single mode (3 μm), double mode (3, 7-13 μm) and triple mode (3, 9-15, 21-25 μm) were observed. The main findings are as follows:

Among all fog cases, radiation fog accounts for the largest proportion. Radiation-advection fog tends to persist longer and is typically associated with trimodal DSDs. Unimodal cases are more likely to occur when the fog duration is short, the DSD is narrow, or the FBS is high. For bimodal and trimodal cases, both the number of peaks and their diameters vary with the fog life cycle. As the fog develops, sustained condensational growth often leads unimodal and trimodal DSDs to evolve into bimodal, with more concentrated peaks. The peak diameters are linked to the ability of fog to maintain high number concentrations and liquid water content. Although the N_f of larger droplets increases, droplets around 3 μm consistently exhibit the highest N_f, indicating continuous activation and formation of new droplets during the condensational growth.

The probability density function (PDF) distributions of microphysical properties vary across spectral modes. For all modal types, the PDF decreases with increasing N_f and LWC. Compared to trimodal DSDs, the PDF distributions of R_v and R_{eff} in bimodal DSDs are more concentrated. The contribution of each bin to N_f aligns well with the appearance of modes, while larger droplets contribute significantly to LWC.

Comparison of the retrieved physical parameters from segmented gamma and lognormal fitting with observations indicates that the three-segment fitting yields the best performance, especially in improving N_f and LWC estimation. Meanwhile, the three-segment fitting reduces the estimation deviations in R_{eff}, absorption coefficient and optical thickness from up to 90% in the non-segmented fitting to below 20%, demonstrating its effectiveness in improving fog DSD representation and microphysical characteristic retrieval.

These findings advance our understanding of fog droplet size distribution (DSD) evolution during fog lifecycles and the correlations between DSD modes and microphysical properties, providing fundamental insights into fog microphysics in polluted urban regions such as the Yangtze River Delta, China. The improved segmented gamma and lognormal fitting offers a new perspective for DSD parameterization and demonstrates strong potential for improving the representation of cloud/fog microphysical processes in weather prediction and climate models.

It should also be noted that in this work, only a three-parameter gamma and lognormal distribution was used to fit and refine the mean DSD. The comparative performance of alternative distribution and evaluate the influence of different parameterizations on fitting accuracy could be explored in future studies."